Laser–Doppler measurements of laminar and turbulent flow in a pipe bend

M. M. Enayet, M. M. Gibson, A. M. K. P. Taylor and M. Yianneskis*

Laser–Doppler measurements are reported for laminar and turbulent flow through a 90° bend of circular cross-section with mean radius of curvature equal to 2.8 times the diameter. The measurements were made in cross-stream planes 0.58 diameters upstream of the bend inlet plane, in 30, 60, and 75° planes in the bend and in planes one and six diameters downstream of the exit plane. Three sets of data were obtained: for laminar flow at Reynolds numbers of 500 and 1093 and for turbulent flow at the maximum obtainable Reynolds number of 43 000. The results show the development of strong pressure-driven secondary flows in the form of a pair of counter-rotating vortices in the streamwise direction. The strength and character of the secondary flows were found to depend on the thickness and nature of the inlet boundary layers, inlet conditions which could not be varied independently of Reynolds number. The quantitative anemometer measurements are supported by flow visualization studies. Refractive index matching at the fluid–wall interface was not used; the measurements consist, therefore, of streamwise components of mean and fluctuating velocities only, supplemented by wall pressure measurements for the turbulent flow. The displacement of the laser measurement volume due to refraction is allowed for in simple geometrical calculations. The results are intended for use as benchmark data for calibrating flow calculation methods.

Keywords: *flow measurement, turbulence, flow visualization, pipe bends*

As a fluid flows through a straight pipe or duct and into a bend the pressure, which in the straight section is uniform across the flow, must adjust in the bend to counter centrifugal forces. The pressure is greatest at the outer wall farthest from the centre of curvature and least at the inner wall nearest the centre of curvature and the cross-stream pressure gradient in the bend has two well known effects on the flow. At the bend inlet, the boundary layer on the outer wall experiences the effects of a positive streamwise pressure gradient which may in a tight bend be sufficiently strong to produce local separation; conversely, the inner wall boundary layer is accelerated. The reverse occurs at the pipe exit where local pressure gradients of the opposite sign appear as the flow adjusts to uniform pressure conditions downstream. Inside the bend, the presence of side wall boundary layers ensures that the conditions for radial equilibrium cannot be satisfied exactly over the entire field. The slow moving fluid in these layers is forced inwards towards the centre of curvature and continuity ensures that the high speed fluid near the axis is driven outwards. The result is a secondary flow superimposed on the main flow.

If the bend is of circular cross-section, or its height is not significantly greater than its width measured in the radial direction, the effect of the secondary flow is to displace the region of maximum velocity from the centre towards the outer wall. If, however, the boundary layers are thin and the secondary flow is weak, the velocity distribution in the inviscid central core will approximate to that of a free vortex with velocity increasing towards the centre of curvature. The effects of longitudinal curvature on the boundary layers on the inner and outer walls also tend to counteract the effects of pressure-driven secondary flow. In the inner boundary layer, the shear stress is reduced by curvature and the boundary layer grows relatively slowly. In the outer boundary layer the shear stress is increased and the layer is retarded and thickened. Thus, in the flow in a high narrow curved channel, where the secondary flows are weak and confined to the edge zones, the region of maximum velocity is found closer to the inner wall[1]. The effects of curvature on laminar boundary layers are weak in ducts of moderate aspect ratio and are masked by the secondary flow; the fractional change in shear stress is of order δ/R (where δ, boundary layer thickness and R, radius of curvature). The effects of curvature on the turbulence

* Fluids Section, Mechanical Engineering Department, Imperial College of Science and Technology, Exhibition Road, London, UK, SW7 2BX
Received 5 March 1982 and accepted for publication on 14 June 1982

in turbulent boundary layer flow are an order of magnitude greater[2] and may be sufficiently large to counteract the effects of secondary flow and to be significant in determining the flow structure.

The presence and origin of secondary flow in bends have long been known and understood although obvious measurement difficulties associated with probe explorations have hindered detailed investigation and have largely restricted experiments to flow visualization studies and measurements of overall pressure loss. The former[3] show that a laminar boundary layer in a 90° pipe bend is deflected through 45° while the deflection of a turbulent layer does not exceed 30°. Work carried out prior to 1970, which consists almost entirely of measurements of wall pressure and pressure probe surveys of the outlet plane, is summarized and reviewed by Ward-Smith[4]. These data provide a basis for empirical pressure decrease correlations but are necessarily too limited to be used for the validation of flow calculation methods. The development of these methods to the point where they can be used as standard design tools has, fortunately, been paralleled by the development of the laser–Doppler anemometer which, by obviating the need for probe insertion, has made possible more detailed measurement of complex flows including those in bends. Humphrey *et al*[5] report measurements of the longitudinal velocity component in laminar flow through a strongly curved duct of square cross-section. This work has been extended[6] to the measurement in turbulent flow of two components of mean velocity, two components of turbulent energy and one shear stress component; similar measurements also have been reported[7] for laminar and turbulent flow with thin inlet boundary layers.

The problem of flow in a round pipe, which is examined in this paper, presents additional measurement difficulties and has consequently received less attention. Rowe[8] reports total-pressure measurements in a mildly curved pipe bend while laser–Doppler measurements appear to be limited to the laminar flow experiment described by Agrawal *et al*[9]. The difficulties arise because in off-diameter planes, the laser beams are refracted at the fluid–wall interface unless care is taken to match the refractive indices. If this is not carried out, the measurements will be limited to longitudinal components of mean and fluctuating velocity. The measurement volume is displaced but to a position which can be located reasonably accurately by simple calculation[10].

In this paper, measurements are reported of laminar and turbulent flow in and downstream of a tight 90° pipe bend. The results, which complement and extend those of previous investigations[5–7] are seen as a useful contribution to the 'data bank' available for the further testing and development of numerical flow calculation methods.

Experimental

Test bend

The geometry and dimensions of the test bend are shown in Fig 1. The dimensions are similar to those of the square-sectioned bend used previously[6,7] with

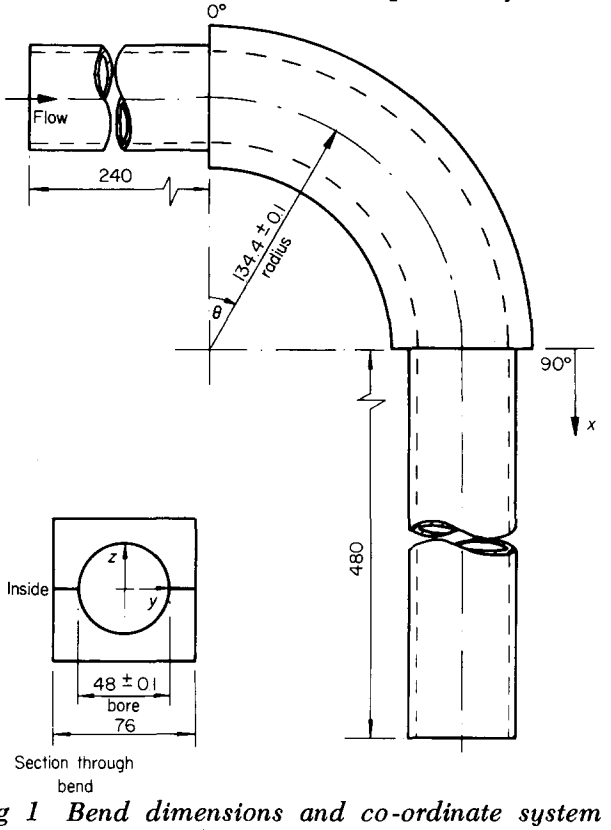

Fig 1 Bend dimensions and co-ordinate system (dimensions in mm)

Notation

C_p	Pressure coefficient (Fig 7)
d	Pipe diameter
l	Distance of control volume from pipe wall along refracted beam path
$\dot{m}$	Mass flow rate
p	Static pressure
p_{ref}	Static pressure one diameter upstream of pipe bend
R	Radius of curvature of the bend
r	Internal radius of pipe $= \frac{1}{2}d$
Re	Reynolds number $U_B d/\nu$
U	Streamwise local mean velocity
U_B	Bulk velocity $4\dot{m}/(\pi\rho d^2)$
u'	rms streamwise velocity fluctuation
x	Distance measured along the pipe and bend centreline
y	Distance measured horizontally from centreline (Fig 1)
z	Distance measured vertically from centreline (Fig 1)
β	half-angle of beam intersection
δ	Boundary layer thickness
θ	Bend angle (Fig 1)
ϕ	Angle subtended at pipe centreline (Fig 7)
ν	Kinematic viscosity
ρ	Density

radius of curvature equal to 2.8 times the internal diameter. The bend was machined accurately from two halves of a rectangular perspex block, split in the plane of symmetry. It was thus possible to maintain a tolerance of ±0.1 mm on the internal diameter and to minimize refraction problems at the external, air–perspex interface by the retention of a rectangular external section. The bend was fixed in the horizontal plane downstream of a straight tube of the same diameter (48 mm) and 240 mm long; a second straight tube, 480 mm long, was fitted downstream.

The bend was fitted in a water flow rig identical to that described by Taylor *et al*[7]. The flow rate was constantly monitored using Fischer and Porter precision flowmeters. The maximum obtainable Reynolds number, $4\dot{m}/\pi\nu d$, was 43 000. For the turbulent flow measurements the water was seeded with minute quantities of milk to increase the scattering particle concentration and, consequently, the particle arrival rate[11].

Instrumentation and signal processing

The optical arrangement is similar to that described by Taylor *et al*[7]. The light beam generated by a 5 mW helium–neon laser is focussed on to a radial diffraction grating, collimated to reduce spherical aberration and then focussed to form the scattering volume at the point of measurement in the bend. Measurements in the vertical plane were made in the straight pipe sections at each end of the bend. For these the light beam was turned through 90° using a mirror which was optically flat to within one tenth of the wavelength of light. Forward scattered light collected by the objective lens is focussed on and passes through a pinhole to an EMI 9658 photomultiplier, the output from which is processed in a Cambridge Consultants CC01 frequency tracking demodulator. The principal characteristics of the laser–Doppler anemometer are given in Table 1.

Scope and accuracy of the measurements

Refraction of the laser beam at the water–perspex interface not only displaces the measurement volume by an amount which can be readily calculated but also, and more importantly, prevents the measurement of cross-section velocity components. The method used successfully for the latter in the rectangular bend experiments[6,7] fails for the round pipe because, unless the refractive indices of the fluid and pipe wall are equal, the twin laser beams entering the pipe in a plane at 45° to the axis cannot converge. Consideration has been given to the use of fluids other than water which would allow the indices to be equalized. Unfortunately, it appears that such fluids either possess highly unpleasant or toxic properties or are so viscous that it is difficult to realize Reynolds numbers high enough for turbulent flow. An example of this is given in the experiment described by Agrawal *et al*[9] where the use of a glycerine–water mixture to match the indices limited the investigation to laminar flow. As the main objective here is the study of turbulent bend flow, the limitation on the scope of the measurements to streamwise velocities only has had to be accepted at this stage.

There is no difficulty in measuring the streamwise velocities or in calculating the displaced position of the measurement volume. The measurements are made at points along the optical axis which is refracted at the pipe wall at an angle to the plane of symmetry to which it was originally parallel. A straightforward calculation produces the beam trajectories shown in Fig 2. The actual location of

Table 1 Optical characteristics of the laser–Doppler anemometer

Focal length of imaging lens	300 mm
Half-angle of beam intersection	9.11°
Fringe separation (line-pair spacing)	1.9 μm
Number of fringes in measuring volume	84
Intersection volume diameter calculated at $1/e^2$ intensity	0.167 mm
Intersection volume length calculated at $1/e^2$ intensity	1.391 mm
Photomultiplier pinhole diameter	0.50 mm
Transfer constant	0.500 MHz/ms

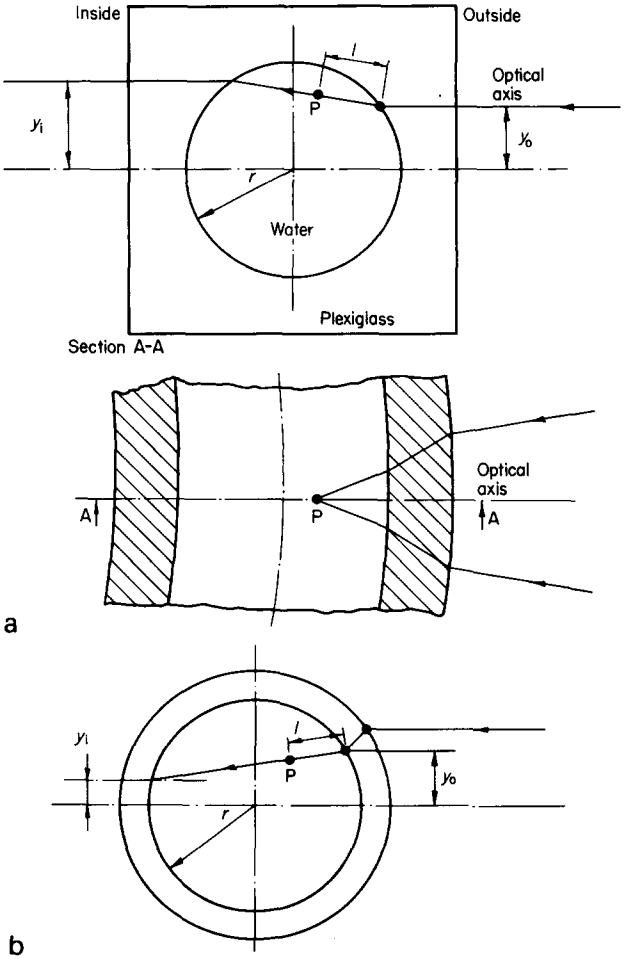

Fig 2 (a) Beam paths through test section. Bend section in θ–y plane. Point P marks location of scattering volume (b) Cross-section through upstream and downstream tangents

the measurement points along the optical axis is obtained by applying the correction described by Boadway and Karahan[10] for the effects of refraction due to the bend curvatures. These two corrections have been applied independently to the results presented here. It was also found that signal quality was only slightly impaired by refraction and that measurements were feasible for points in the flow distant more than one tenth of the radius from the wall in the vertical plane.

Estimated measurement errors are summarized in Table 2. Corrections were not applied for the effects of finite transit time and instrument noise broadening. Systematic errors of up to 2.5% are mainly associated with velocity gradient effects near the walls and have been included in the Table.

The measurements were made in cross-stream planes 0.58 diameters upstream of the bend inlet plane, in 30, 60, and 75° planes in the bend and in planes at one and six diameters downstream of the exit plane. Three sets of data were obtained: for laminar flow at Reynolds numbers of 500 and 1093 and for turbulent flow at the maximum obtainable Reynolds number of 43 000.

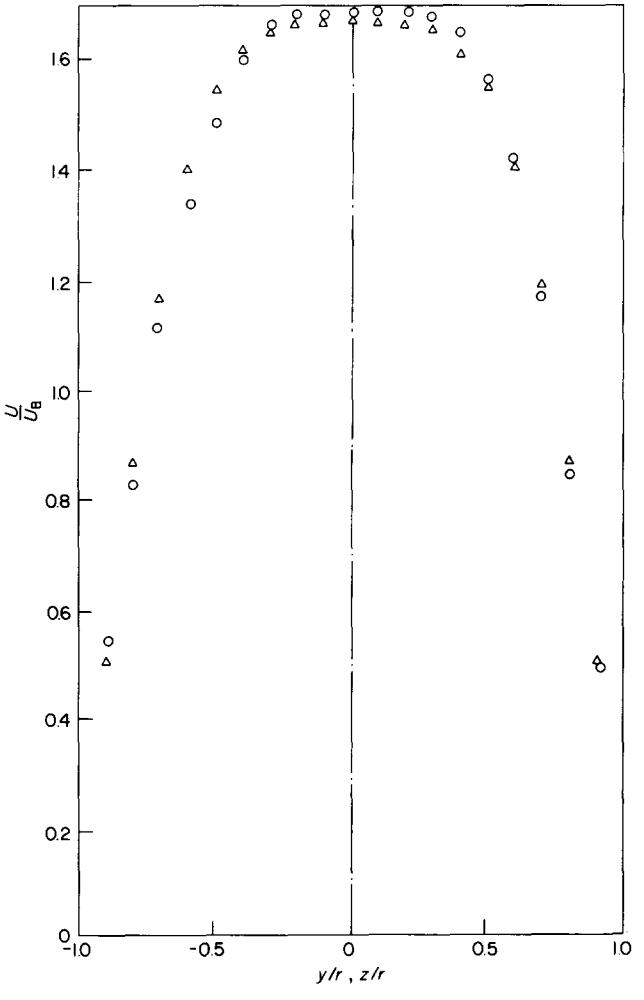

Fig 3 Horizontal, ○, and vertical, △, profiles of mean velocity in the laminar approach flow 0.58 diameters upstream of the inlet plane. Re = *500*

Results and discussion

Flow visualization

Observation of hydrogen bubble paths in low speed flow revealed no unusual features such as the local separation reported[5] for fully developed flow through the square-section bend. These observations were entirely consistent with large-scale secondary flow patterns detected by laser-Doppler anemometry.

Laminar flow measurements

The results of velocity measurements at a Reynolds number of 500, mean velocity 10·5 mm/s, are shown in Figs 3 and 4. Fig 3 shows the inlet conditions: horizontal and vertical velocity profiles 0.58 diameters upstream of the bend. The boundary layer thickness is $\approx 0.27\,d$ so that there is a significant potential core. The apparent, slight asymmetry shown in the results is within the estimated error band. Contours of the streamwise velocity in four cross-stream planes (Fig 4) show the effects of strong secondary flow which displaces the region of maximum velocity to the outside of the bend. The secondary flow develops gradually: in the 30° plane the only visible effect is a thickening of the shear layer on the inside of the bend. By 60° the secondary flow has become almost fully developed as is shown by the distortion of the contours. The fourth set of

Table 2 Measurement errors

Quantity	Systematic error	Random error
x	±0.5 mm	±0.02 mm
y, z	±0.2 mm	±0.02 mm
θ	±0.3°	±0.17°
β	±0.05°	nil
U_B (laminar)	±0.8%	±0.8%
U_B (turbulent)	±1.5%	±0.5%
U/U_B	up to 2.5%	±1.5%
u'/U_B	up to 3%	up to ±3%

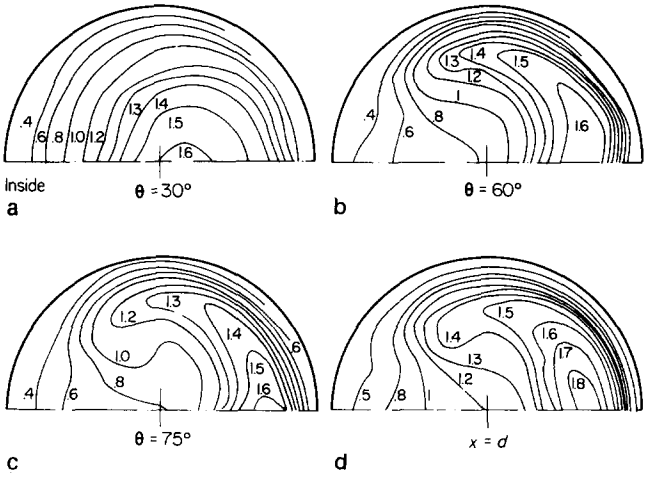

Fig 4 Contours of mean velocity U/U_B *in the bend, laminar flow* Re = *500*

contours, in the plane one diameter downstream, shows that the secondary motion persists without significant decay to this distance.

The effects of doubling the mean velocity and Reynolds number to 23 mm/s and 1093, respectively, are shown in Figs 5 and 6. The inlet boundary layers are reduced in thickness by ≈15% to 0.23 d, the transverse pressure gradient is increased and the secondary flow is intensified. The peak velocity in the 30° plane is displaced from the plane of symmetry but remains closer to the centreline. This displacement, which persists downstream, has also been observed in the flow in a square bend[7]. The shape of the contours near the outside of the bend reflect scatter in the data attributable mainly to difficulties in locating accurately the measurement volume near the wall and partly, perhaps, to slight asymmetry in the flow.

In neither case do the measurements show any unexpected feature: the secondary flow superposed on the main motion is essentially as described qualitatively elsewhere[1,3]; it develops gradually and persists downstream after the removal of the transverse pressure gradient responsible for its generation in the bend. The strength and location of the pressure-driven secondary flow depend on the inlet conditions and the Reynolds number which could not be varied independently in these experiments. The stronger secondary flow observed at $Re = 1093$ must be attributable mainly to the increased centrifugal forces and transverse pressure gradient rather than to the relatively small changes noted in the initial conditions. These quantitative data of velocity in the bend are considered to be sufficiently accurate to be useful in checking the numerical accuracy of flow prediction methods.

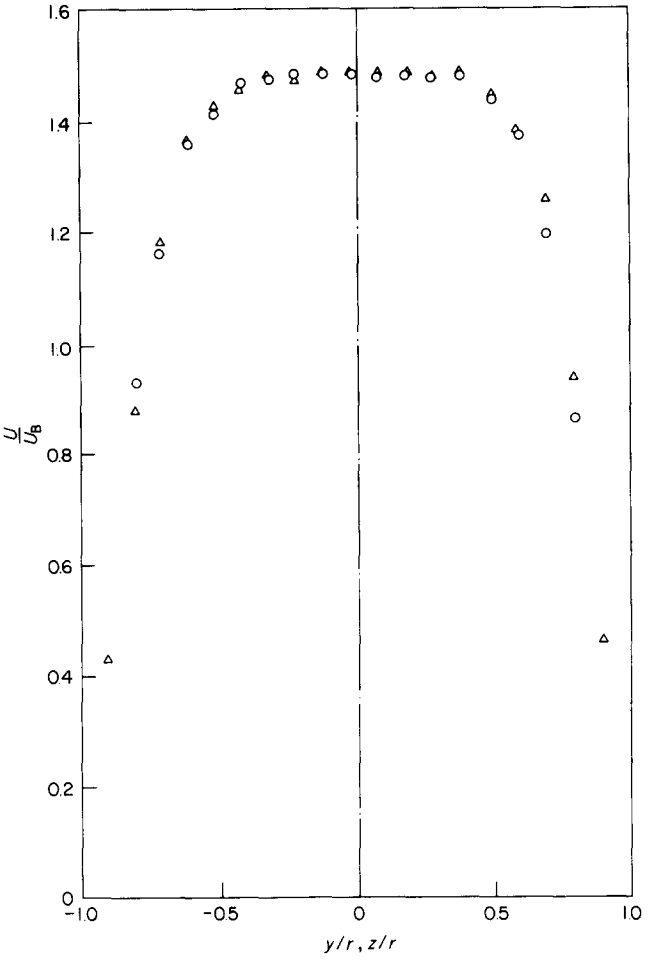

Fig 5 Horizontal, ○, and vertical, △, profiles of mean velocity in the laminar approach flow 0.58 diameters upstream of the inlet plane, Re = *1093*

Turbulent flow measurements

At the maximum flow velocity of 0.92 m/s, Reynolds number 43 000, the inlet boundary layers are turbulent. The static pressure variation on the bend wall is large enough to be measured accurately with the results shown in Fig 7. At the bend inlet, the negative pressure gradient on the inner wall is approximately twice the positive gradient on the outside. These initial gradients resulting from the change from straight to curved flow disappear at ≈25° so that in the mid-section of the bend ($25° < \theta < 75°$), a quasi-equilibrium condition is reached with approximately uniform pressure on the inner and outer walls. The transition to straight flow downstream is signalled by the appearance of strong gradients for $\theta > 75°$. The overall pressure decrease is about $0.3\rho U_B^2$.

Laser–Doppler measurements of the mean and rms fluctuation of the streamwise velocity at inlet are shown in Fig 8 and contours of these quantities at downstream stations in Figs 9 and 10. The inlet boundary layers of Fig 8 are much thinner, 0.09 d, than in the two laminar flows investigated and the presence of a large central region of uniform velocity flow influences significantly the development of secondary flow downstream. The mean velocity contours (Fig 9) show that by the 30° plane the potential

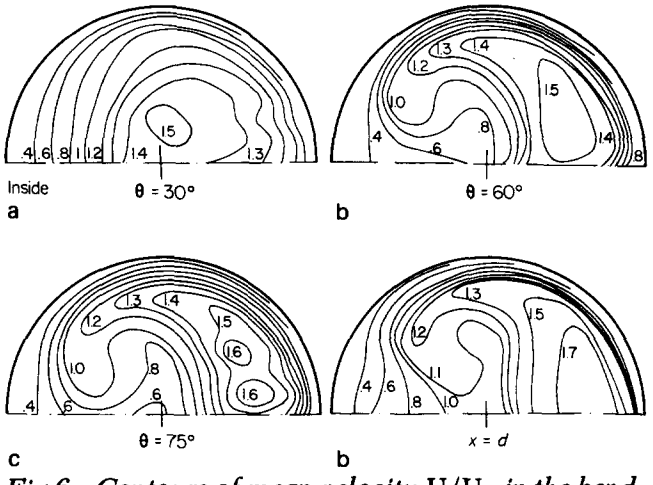

Fig 6 Contours of mean velocity U/U$_B$ *in the bend, laminar flow,* Re = *1093*

core has adjusted to the cross-stream pressure gradient imposed by the bend and the region of maximum velocity has been displaced toward the inside. The results also differ from the corresponding laminar flow measurements in that the thickness of the outer wall boundary layer is increased relative to that on the inside of the bend due mainly to the effects of the potential flow adjustment and the wall

pressure gradients of opposite sign but also, quite possibly, to the effects of longitudinal curvature on the turbulence structure. In the 60° plane, distortion of the contours suggests the presence of strong secondary flow largely confined to the region of steep velocity gradients near the inner wall. This secondary flow grows with distance through the bend and by the 75° plane extends over and beyond the inner half of the section. The removal of the transverse pressure gradient in the straight flow downstream results in a shift of the velocity maximum toward the outside. A large secondary flow, similar to that observed in the laminar flow experiments, now extends over the entire flow area and persists in the plane six diameters downstream of the bend where, however, the transverse velocity gradients have decayed to approximately one half of their values one diameter downstream.

The contours of turbulence intensity (Fig 10) are consistent with those of the mean velocity. As expected, high values of the velocity fluctuation are associated with steep mean velocity gradients and with the distortion of the symmetrical inlet flow.

These results may be compared with the measurements made by Humphrey *et al*[6] in a tight

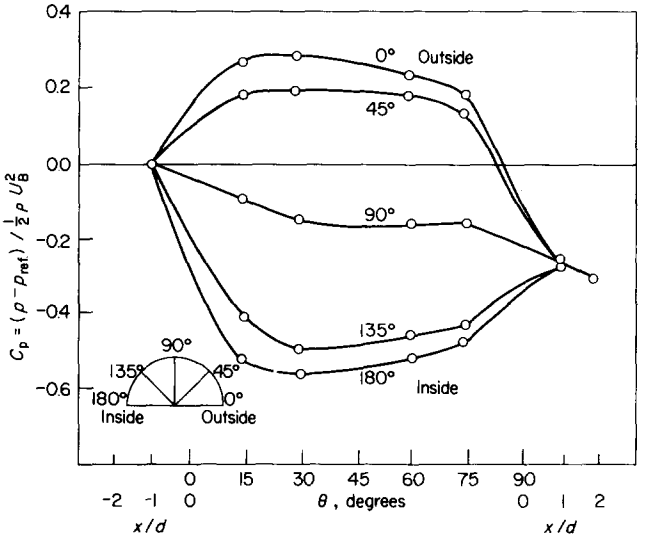

Fig 7 Wall static pressure variation. Turbulent flow Re = *43 000*

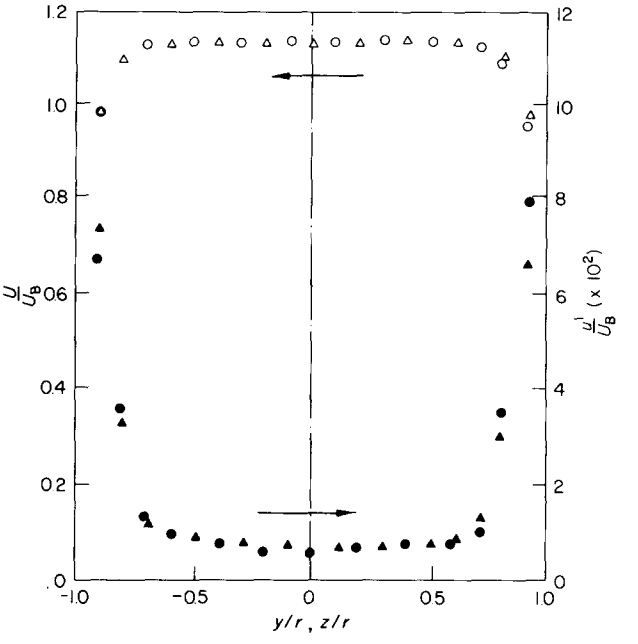

Fig 8 Profiles of mean velocity U/U_B *and turbulence intensity* U'/U_B *in the turbulent approach flow 0.58 diameters upstream of the bend.* ○ *horizontal,* △ *vertical,* Re = *43 000*

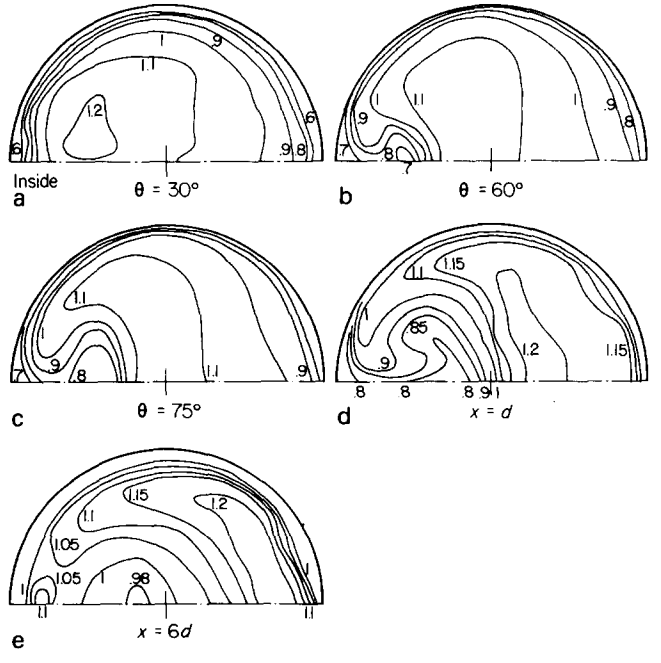

Fig 9 (a–c) Contours of mean velocity U/U_B *in the bend. (d–e) Contours of mean velocity* U/U_B *downstream of the bend. Turbulent flow,* Re = *43 000*

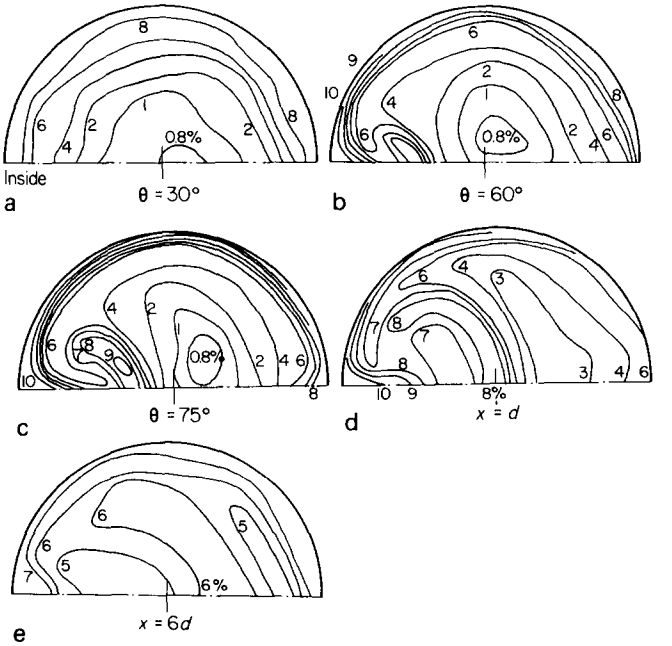

Fig 10(a–c) Contours of turbulence intensity (u'/U_B) *in the bend. (d–e) Contours of turbulence intensity* (u'/U_B) *downstream of the bend. Turbulent flow,* Re = *43 000*

bend of square cross-section. The inlet boundary layers of that flow were substantially thicker than the flow here and contained stress-driven secondary flows towards the corners. Consequently, the pressure-driven secondary flow was similar to those observed in the two laminar flows and extended over the entire flow area.

Conclusions

The measurements show, as expected, that in bend flow, strong cross-stream flows occur which are produced by the inward motion of slow moving fluid in a radial pressure gradient. The strength of the secondary flow is influenced by the initial inlet flow conditions: when the inlet boundary layers are thin, as in the turbulent flow case reported here, the initial flow adjustment is an inward shift of the velocity peak in the potential core. The secondary flow then develops initially in the inside of the bend. The secondary flow always takes some time to develop and its effects are still increasing by the exit and persist downstream.

The effects of refraction at the doubly-curved fluid–wall interface prevent the measurement of cross-stream velocity components. The investigation of flows in the round bend to the same level of detail that has been achieved previously in square bends, will require refractive index matching. For the streamwise velocity measurements reported here, simple geometrical corrections allow for the displacement of the measurement volume by refraction.

The laminar flow data may be used to check the numerical accuracy of flow prediction methods; the turbulent flow measurements provide the additional information needed to validate mathematical models of turbulence.

Acknowledgements

This research was supported principally by a research contract from the CEGB Central Electricity Research Laboratories, UK. A. Taylor and M. Yianneskis received financial support from NASA Lewis Research Center, USA. Professor J. H. Whitelaw contributed valuable advice in numerous discussions. Mr O. Vis made the test bend, Mr M. Roper the water channel and Miss K. Maxwell prepared the typescript.

References

1. **Goldstein S.** (ed). Modern developments in fluid dynamics. *Oxford, 1938*
2. **Bradshaw P.** Effects of streamline curvature on turbulent flow. *AGARDograph 169, 1973*
3. **Prandtl L.** Essentials of fluid dynamics. *Blackie, London, 1952*
4. **Ward-Smith A. J.** Pressure losses in ducted flows. *Butterworth, London, 1971*
5. **Humphrey J. A. C., Taylor A. M. K. P. and Whitelaw J. H.** Laminar flow in a square duct of strong curvature. *J. Fluid Mech. 1977,* **83**, *509*
6. **Humphrey J. A. C., Whitelaw J. H. and Yee G.** Turbulent flow in a square duct with strong curvature. *J. Fluid Mech., 1981,* **103**, *443*
7. **Taylor A. M. K. P., Whitelaw J. H. and Yianneskis M.** Measurements of laminar and turbulent flow in a curved duct with thin inlet boundary layers. *NASA Contractor Rep. 3367, 1981*
8. **Rowe M.** Measurements and computations of flow in pipes. *J. Fluid Mech., 1970,* **43**, *771*
9. **Agrawal Y., Talbot L. and Gong K.** Laser anemometry study of flow development in curved circular pipes. *J. Fluid Mech., 1978,* **85**, *497*
10. **Boadway J. D. and Karahan E.** Correction of laser Doppler anemometer readings for refraction at cylindrical interfaces. *DISA Information 26, 1981*
11. **Durst F., Melling A. and Whitelaw J. H.** Principles and practice of Laser–Doppler anemometry. *Academic Press, London, 1976*

Letter to the Editors

Second law debate

Dr Kotas' attempted rebuttal in your September issue (Vol 3, No 3) of my reply to his criticism of my book Thermodynamic Principles of Energy Degrading can be shown to be ludicrous, undoubtedly due to his almost complete lack of comprehension of what I have attempted to do in a simple treatment of this important subject.

If he will read my first reply to his original review, he will note the sentence: "This heat transfer can be thought of as occurring *very rapidly* after the work interaction (and therefore *under entirely different conditions* compared with the real combined process) provided that the same end state is reached". In the example of an isothermal expansion process with fluid friction but without heat transfer irreversibility, he has deliberately taken the subsequent heat transfer process a-2 as occurring at the isothermal temperature T_R. Naturally, this distortion leads to an erroneous conclusion, and may I suggest respectfully that Dr Kotas need not have gone to the trouble of choosing an isothermal process at all since the original Fig 6.4 serves adequately to illustrate that such an interpretation is not only erroneous but also ridiculous. Quite simply, I have stated before and I will repeat that any process can be thought of as consisting of an adiabatic followed by one wherein the *same* heat Q as that which flowed in the original process is assumed to occur extremely rapidly until the same final condition is reached. The ΔQ_{unav} defined in Fig 6.4 and in my book is that which pertains to this subsequent and extremely rapid heat transfer process and is therefore not at all zero, even though in Dr Kotas' example the original process is externally reversible.

Such an interpretation, in fact, can be the only one which makes Fig 6.4 valid at all, and I would have thought that Dr Kotas would have perceived this immediately. For in this particular case, the extremely rapid heat transfer of the second process a-2 would have made T_R in the figure very high, and ΔQ_{unav} would then equal I_{ext} as illustrated in the combined diagram. This can be the only interpretation of the combination technique which makes it at all viable.